J Supercond Nov Magn (2011) 24:2153–2159
DOI 10.1007/s10948-011-1174-9

ORIGINAL PAPER

Investigation of Gd Addition Added on Magnetic and Structural Properties of $Bi_{1.8}Pb_{0.35}Sr_{1.9}Ca_{2.1}Cu_3Gd_xO_y$ Superconductors by ac Susceptibility

G. Yildirim · Y. Zalaoglu · M. Akdogan · S.P. Altintas · A. Varilci · C. Terzioglu

Received: 1 February 2011 / Accepted: 7 April 2011 / Published online: 6 May 2011

Abstract This study reports the effect of Gd addition on magnetic and structural properties of $Bi_{1.8}Pb_{0.35}Sr_{1.9}Ca_{2.1}Cu_3Gd_xO_y$ superconductor with $x = 0, 0.1, 0.2, 0.3, 0.4$ and 0.5 by means of ac susceptibility measurements at various ac fields (ranging from 270 to 1352 A/m) and scanning electron microscopy (SEM) images. Critical onset (T_c^{on}) and loss peak temperatures (T_p) were qualitatively estimated from the ac susceptibility curves. The peak temperature at zero ac-magnetic field (T_{p0}) and intergrain critical current densities (J_c) were theoretically calculated from the ac susceptibility plots via the critical state models. The results show that peak temperatures and critical current densities were found to decrease with increasing Gd addition. Moreover, using a self-field approximation together with J_c dependence on temperature, the characteristic length (L_c) associated with the pinning force is estimated to be approximately the same as the average grain size (R_g) of the pinning center because of the linear decrease in J_c with increasing temperature. Surface morphology and grain connectivity of the samples were also obtained to degrade with increase in the Gd addition from SEM investigations.

Keywords $Bi_{1.8}Pb_{0.35}Sr_{1.9}Ca_{2.1}Cu_3Gd_xO_y$ · Ac susceptibility · Critical state models · Critical current density · Peak temperature · Scanning electron microscopy

G. Yildirim · M. Akdogan · S.P. Altintas · A. Varilci · C. Terzioglu
Department of Physics, Abant Izzet Baysal University, Bolu 14280, Turkey

Y. Zalaoglu (✉)
Department of Physics, Osmaniye Korkut Ata University, Osmaniye 80000, Turkey
e-mail: yzalaoglu@osmaniye.edu.tr

1 Introduction

Researches on Bi-based superconductors $Bi_2Sr_2Ca_{n-1}Cu_nO_x$ ($n = 1, 2, 3$) discovered by Maeda et al. [1] increase [2–7] day by day owing to the fact that the interest in both the fundamental research and applications in technology and industry of these materials in the last decades stems from their remarkable smaller power losses, high current and magnetic field carrying capacity, optical and electronic properties [8–11]. For years, researchers have tried to improve their superconducting properties by using several techniques [12–20]. The improvement of the critical current density means the enhancement of trapped flux in the superconductor material [21, 22] and single domain structure [23, 24]. Likewise, the increase in the critical temperature means the enhancement of average Cu valency, and so the density of mobile holes in the CuO_2 planes [25] containing the magnetic Cu^{2+} ions probably improve the superconductivity [26]. However, these techniques may sometimes cause to decrease the number of charge carriers (either holes or electrons) in the sample and thus the superconducting properties might be suppressed. To illustrate, when the Ca^{2+} ions are replaced by Gd^{3+} ions, the formal Cu valence will decrease [27], hence T_c of the material will tend to decrease. As can be understood, the replacement of Ca^{2+} by Gd^{3+} ions decreases the density of mobile holes in the CuO_2 and degrades the superconductivity. In this study, the effect of concentration of Gd^{3+} ions on structural and magnetic properties of Bi-2223 superconductor was clearly pointed out by ac susceptibility measurements (χ' and χ''). These measurements, covering the dynamic response of superconducting materials since the contactless measurements of specimen susceptibility, show detailed information on superconducting properties such as critical current density, pinning strength, flux creep, activation energy and volume fraction

of grains. T_c^{on}, T_p, T_{p0} and J_c were determined using critical state models [28–33]. The results show that the superconducting properties of the samples were found to decrease with increasing Gd addition. Moreover, using a self-field approximation together with J_c dependence on temperature [34, 35], the characteristic length (L_c) associated with the pinning force in relation to the average grain size (R_g) of the samples is estimated. Surface morphology and grain connectivity of the samples were also interpreted by SEM investigations. Based on the results, superconducting parameters, morphology and grain connectivity of the samples degrade with increasing Gd content.

2 Experimental Details

The starting materials in this work were commercially available powders of Bi_2O_3, PbO, $SrCO_3$, $CaCO_3$, CuO and Gd_2O_3 (Alfaaesar Co., Ltd. 99.9% purity). Superconducting $Bi_2Pb_1Sr_2Ca_{2.2}Cu_{3.2}O_x$ materials were prepared by the standard solid-state reaction method. These oxides and carbonates were weighed in stoichiometric proportion and mixed in a grinding machine for 24 hours to obtain homogeneous mixture. After milling process, the homogeneous mixture of powders was subjected to calcination process at 800 °C for 24 hours in a furnace at 10 °C per minute heating rate. After calcinations process, the resultant powder was pressed into rectangular bars with dimensions of 10 mm × 4 mm × 2 mm at 330 MPa. The sintering process was carried out at 830 °C for 48 hours in the tube furnace with different Gd additions of $x = 0, 0.1, 0.2, 0.3, 0.4, 0.5$ in $Bi_{1.8}Pb_{0.35}Sr_{1.9}Ca_{2.1}Cu_3Gd_xO_y$. The heating and cooling rates of the tube furnace were chosen to be 10 and 3 °C/min, respectively. Hereafter, we will use the abbreviations Gd0, Gd1, Gd2, Gd3, Gd4 and Gd5, respectively. All the calcinations and sintering processes of the samples were performed by using a programmable tube furnace (Protherm-Model PTF 12/75/200). For comparison, an undoped sample was also subjected to the same annealing conditions.

The ac susceptibility measurements on the samples were performed using a home-made susceptometer and a lock-in amplifier (Stanford Research SR850) as was seen in Ref. [36]. The susceptometer consists of a drive coil to apply ac magnetic field, a thermocouple to measure the temperature and a heater to heat the sample from 4 to 120 K. The heater was wounded with doubled wire to eliminate the magnetic field contribution. The temperature measurement was performed by Cu-constantan thermocouple, which was in contact with the sample. The uncertainty of temperature measurements was found to be about 0.02 K. The sample was placed in a vacuum-sealed Pyrex tube, which was then evacuated by a vacuum pump. Following the evacuation, He gas was transferred into the Pyrex tube as heat exchange medium. Pressure of He gas was about 1 bar. The measurements started at 4 K with heating rate of 1 K/min in the temperature range 4–120 K. We used ac field amplitudes of 270, 540, 811, 1082 and 1352 A/m and we fixed frequency at 1000 Hz. At the completion of each measurement, the applied magnetic field was removed at 125 K in order to reduce the trapped field in the sample. Lake Shore 332S-T1 temperature controller was used for temperature sweeping. Susceptibility data taken from lock-in amplifier were recorded using the Labview computer software. Moreover, Tegam, model 73, precision ratio transformer was used as an amplifier because of the fact that the signal generated was very weak. Structural characterization was also performed by Scanning Electron Microscopy (JEOL 6390-LV). Based on the scanning electron micrographs, we estimated the average grain size of the samples.

3 Results and Discussion

3.1 Ac Susceptibility and Intergranular Peak Temperature

As it is well known from literature, ac susceptibility measurements are a strong tool to infer information about the diamagnetic onset temperature, flux dynamics and surface shielding of the materials [37]. In this respect, χ'–T curve of a high-T_c sample shows the diamagnetic onset temperature and shielding fraction of the superconducting phases whereas the χ''–T curve presents the dynamics of flux penetration into the superconductor.

Figure 1, displaying the ac susceptibilities (χ' and χ'') versus temperature graphs, reveals that onset temperatures (T_c^{on}) were observed to be about 110 K for Gd0, 89 K for Gd1, 81 K for Gd2, 76 K for Gd3, 56 K for Gd4 and 40 K for Gd5 sample respectively. On the other hand, the loss peak temperatures (T_p), representing the full flux penetration in the out of phase component of the samples, are noted to be about 105 (93) K for Gd0, 84 (71) K for Gd1, 77 (66) K for Gd2, 71 (59) K for Gd3, 44 (33) K for Gd4 and 30 (19) K for Gd5 at 270 (1352) A/m ac field, respectively.

As can be seen from Table 1, T_c^{on} and T_p temperatures are obtained to decrease with increasing Gd addition. This dramatic decrease in T_p of the Gd4 and Gd5 samples was observed with increasing field. Indeed, T_p of the Gd5 is found to be about 19 K at 1352 A/m field. According to these results, the peak of χ'' curve is clearly indicated to be field-dependent because of the pinning hysteretic losses [38]. In addition, the height and width of the intergranular peaks are observed to increase with increasing field, indicating the field penetration (because of the inhomogeneities and granular quality) and the hysteretic losses for the motion of Abrikosov vortices between the grains [28, 29]. The granular quality of the samples is obtained to degrade with increasing the Gd addition. Moreover, the Gd addition is

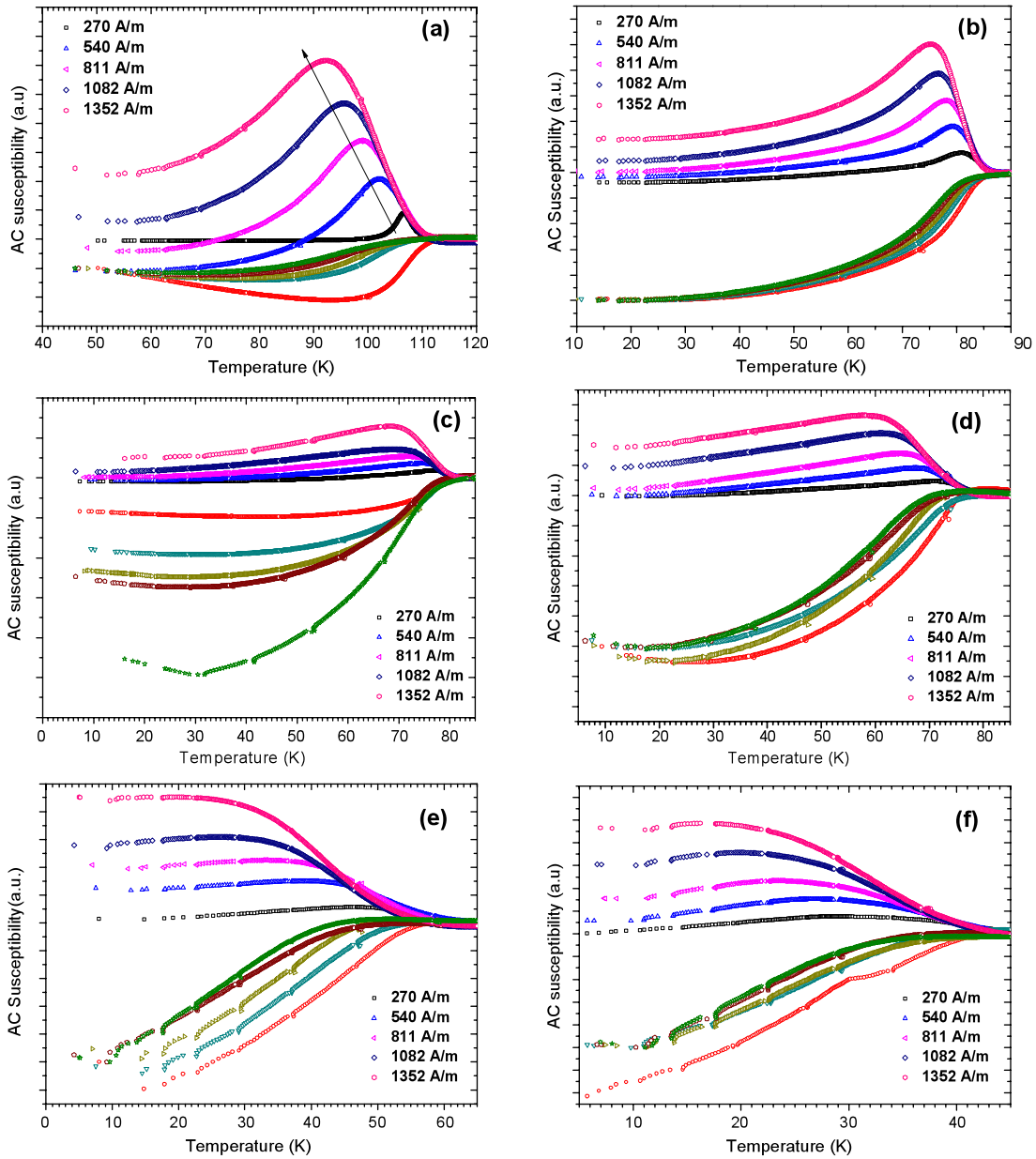

Fig. 1 Real and imaginary parts of ac susceptibility versus temperature plots for (**a**) Gd0, (**b**) Gd1, (**c**) Gd2, (**d**) Gd3, (**e**) Gd4 and (**f**) Gd5

Table 1 T_c^{on} and T_p temperature of Gd0, Gd1, Gd2, Gd3, Gd4 and Gd5 samples at different fields

Samples	T_c^{on} (K)	T_p (K)				
		270 A/m	540 A/m	811 A/m	1082 A/m	1352 A/m
Gd0	110.12	104.62	101.95	99.11	95.67	92.58
Gd1	88.78	83.83	79.47	78.02	75.68	71.14
Gd2	80.94	76.99	74.67	71.63	68.23	65.88
Gd3	75.49	71.02	65.72	64.39	61.91	59.08
Gd4	56.42	43.56	40.01	36.36	34.85	32.94
Gd5	39.78	29.66	26.88	24.35	21.86	19.24

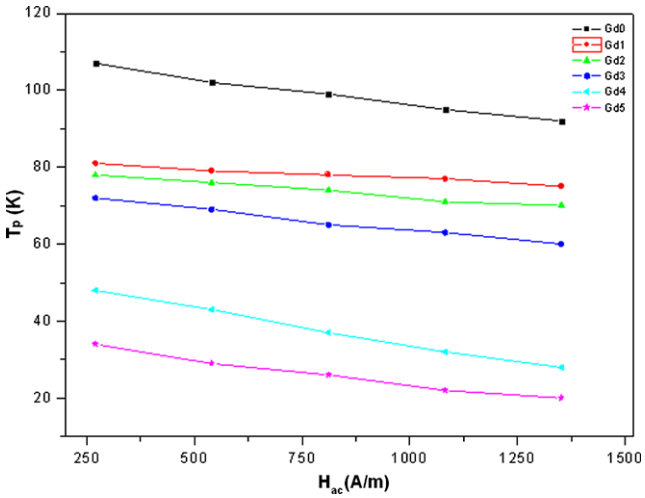

Fig. 2 Intergranular peak temperature vs ac-magnetic field amplitude for the Gd0, Gd1, Gd2, Gd3, Gd4 and Gd5 samples (*solid lines* drawn are only guide to the eye)

noted to cause a broadening of the transition and a reduction of superconducting volume fraction. As a result, the magnitudes of superconductivity properties (i.e. the magnitude of diamagnetism, J_c, T_c^{on}, T_c ($\rho = 0$), T_p and T_{p0}) are found to decrease with the increase of Gd addition.

In order to study the effect of Gd addition on the intergranular pinning force, the loss peak temperature dependence of the imaginary curves as a function of ac-magnetic field (H_{ac}) was investigated. Figure 2 depicts the ac-magnetic field dependence of loss peaks, T_p, for the samples produced. By adopting the critical state model, Muller et al. [39] proposed that T_p is linearly proportional to H_{ac} but inversely proportional to the intergranular pinning force density:

$$T_p = T_{p0} - T_{p0} U^{1/2} H_{ac} \tag{1}$$

where U is $[\mu_0 \mu_{eff}(0)/2a\alpha_J(0)]$, a is the length of the samples, $\mu_{eff}(0)$ is the effective permeability of the ceramic and $\alpha_J(0)$ is the intergranular pinning force density. As seen from Fig. 2, each set of data shows an excellent linear relationship between T_p and H_{ac}. The slope of each line is proportional to $(\alpha_J(0))^{-1/2}$ and the vertical intercept of each line corresponds to the peak temperature, T_{p0}, at zero ac-magnetic field amplitude. From a least-squares fitting procedure by using (1) the data T_{p0} and U were estimated for all samples and are depicted in Table 2.

As seen from the table, the values of T_{p0} and U were found to decrease with increasing Gd addition. The decreasing trend in U means that the values of $\alpha_J(0)$ increase with increase in the Gd addition because of the inverse ratio between U and $\alpha_J(0)$ [36], whereas the decreasing trend in pinning force of the samples with increasing Gd addition can be explained by greater voids and defects.

Table 2 The extracted values of T_{p0}, and U of the Gd added samples

Samples	T_{p0} (K)	U $((\alpha_J(0))^{-1/2})$
Gd0	107.891	2.59×10^{-4}
Gd1	86.869	1.96×10^{-4}
Gd2	80.171	1.53×10^{-4}
Gd3	74.313	1.52×10^{-4}
Gd4	49.191	1.43×10^{-4}
Gd5	35.434	1.33×10^{-4}

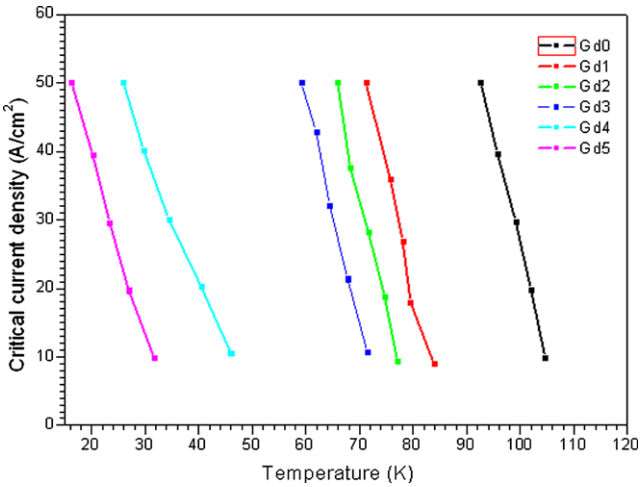

Fig. 3 J_c vs. T_P behavior for (**a**) Gd0, (**b**) Gd1, (**c**) Gd2, (**d**) Gd3, (**e**) Gd4 and (**f**) Gd5 samples (*solid lines* drawn are only guide to the eye)

3.2 Critical Current Density

Temperature-dependent intergranular critical current density J_c (T) in the Gd-doped samples can be estimated by means of critical state models [28–32]. According to Bean model [30, 40], the intergranular critical current density at the peak temperature T_p can be written as $J_c(T_p) = H_a/a \approx H_a/\sqrt{ab}$, where the cross section of the rectangular bar sample is $2a \times 2b$ ($a < b$), J_c is the intergranular critical current density at T_p, the temperature of the χ'' peak, H_a is the amplitude of the applied ac field. The calculated values of J_c for the samples are depicted in Fig. 3. Magnetically estimated critical current densities for only intergrain region at temperatures close to T_c region are plotted because the intergrain peaks have not appeared during the measurements.

From Fig. 3, it seems to be a regression in the intergranular critical current density estimated near the T_c value of the samples with the increase of the Gd addition. This phenomenon can be interpreted on the basis of the regression in the superconducting anisotropy factor, studied in detail in Ref. [41]. Moreover, decrease in the lattice parameter c was clearly revealed with increasing Gd addition [41]. In other words, when the Ca^{2+} ions are replaced by Gd^{3+} ions, T_c of the material decreases because of the decrease in the for-

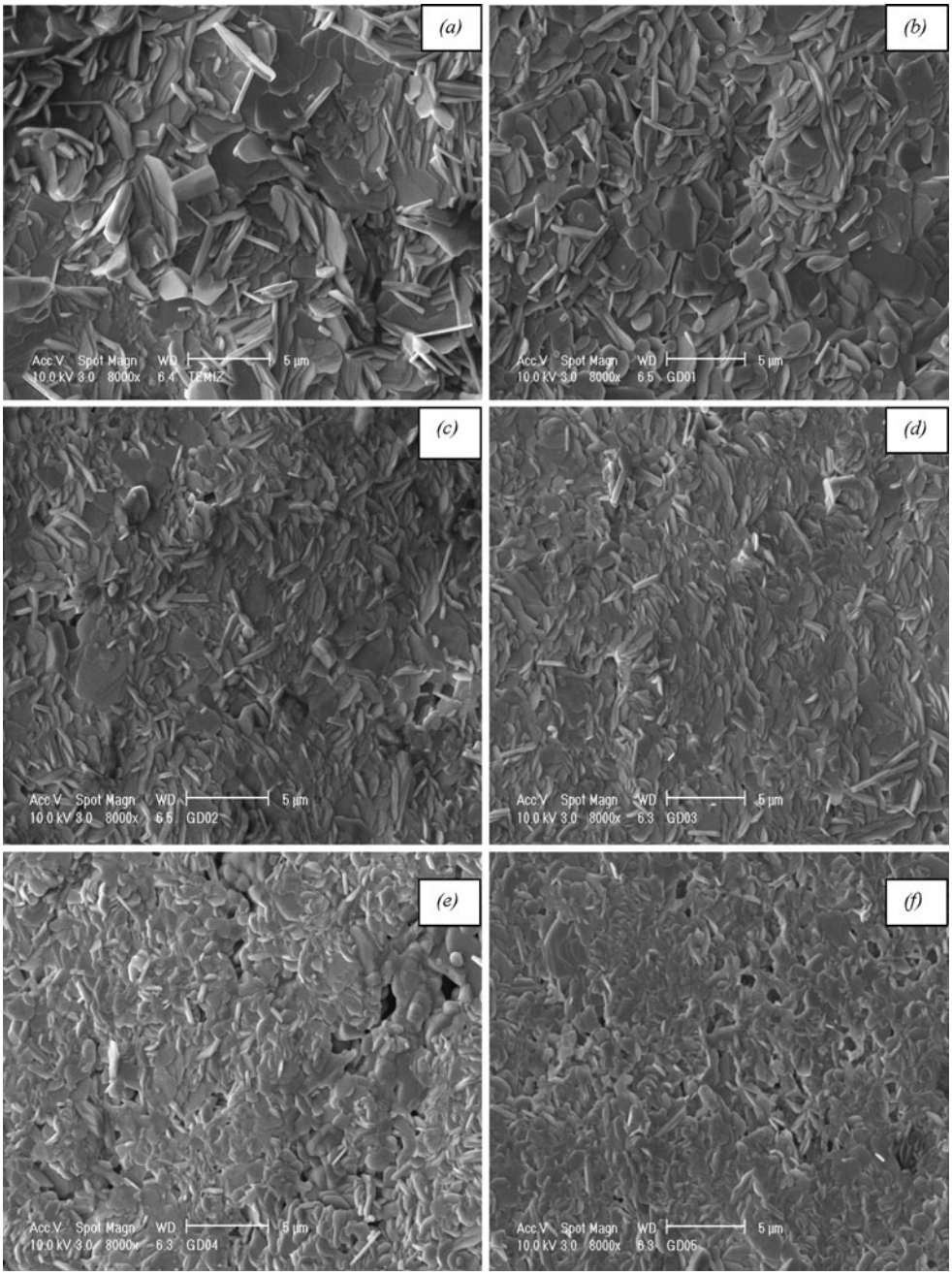

Fig. 4 SEM micrographs of (**a**) Gd0, (**b**) Gd1, (**c**) Gd2, (**d**) Gd3, (**e**) Gd4 and (**f**) Gd5 samples

mal Cu valence. This causes a decrease in the c parameter and magnitude of superconductivity properties. In this study, the Gd0 sample was found to have higher J_c (50 A/cm^2 at 92 K) than the other doped samples (Fig. 3). Moreover, J_c was theoretically obtained to be about 341, 282, 273, 230, 91 and 77 A/cm^2, respectively, at 4.2 K. These results indicate that J_c dramatically decreases with increasing Gd addition. Furthermore, the curve of J_c versus temperature is also an important graph to understand the relationship between the characteristic length and size of the pinning center [42]. In this study, J_c was also found to linearly decrease with increasing temperature as a consequence of thermally activated flux creep. Therefore, the characteristic lengths associated with the pinning force were estimated to be approximately the same as the average grain size of the pinning center.

3.3 SEM Analyses

The surface morphology of the Gd0-Gd5 samples was performed by Scanning Electron Microscopy (SEM). The mi-

crographs in Fig. 4 show that not only is the grain connectivity worsened considerably but also the average crystallite size becomes smaller and smaller with increasing the Gd addition.

In addition, SEM photograph of the Gd0 sample presents a broad grain size distribution and the best crystallinity in comparison with the others. Moreover, the surface of the Gd0 is observed to be more uniform with a better alignment of grains. On the other hand, the Gd5 sample is noticed to have the worst appearance among these samples and there are voids and signs of partial melting on the micrograph of the Gd5. Using image processing, the average grain sizes were also obtained to be about 552, 486, 459, 439, 421 and 408 nm for the Gd0, Gd1, Gd2, Gd3, Gd4 and Gd5 samples, respectively. In conclusion, the surface morphology, grain connectivity and size of the samples were found to degrade from SEM investigations with increasing the Gd addition. These findings were ascertained by ac susceptibility results.

4 Conclusion

Gd-added $Bi_{1.8}Pb_{0.35}Sr_{1.9}Ca_{2.1}Cu_3Gd_xO_y$ samples were prepared by the standard solid–state reaction method with $x = 0$, 0.1, 0.2, 0.3, 0.4 and 0.5, respectively. The magnetic field effect on hysteretic ac losses of the samples was analyzed by using ac susceptibility measurements, from which J_c, T_c^{on}, T_p, T_{p0}, and U values were theoretically determined by means of the critical state models. The results show that not only was the peak of χ'' curve obtained to be field-dependent for pinning hysteretic losses, but also T_c^{on}, T_p, T_{p0}, and J_c were found to decrease with increasing the Gd addition. Based on the linear decrease in J_c with increasing temperature, the characteristic length associated with the pinning force was interpreted to be approximately the same as the average grain size of the pinning center. Furthermore, the grain connectivity is worsened greatly and the average crystallite size becomes smaller and smaller with increasing the Gd addition. As a result, superconducting properties were noticed to decrease with the increasing Gd addition, which has an essential effect on the translation temperature, peak temperature, critical current densities, surface morphology and grain connectivity of the samples. In conclusion, this study reports the clear effect of Gd addition on magnetic and structural properties of $Bi_{1.8}Pb_{0.35}Sr_{1.9}Ca_{2.1}Cu_3Gd_xO_y$ superconductor.

References

1. Maeda, H., Tanaka, Y., Fukutomi, M., Asano, T.: Jpn. J. Appl. Phys. **27**, L 209 (1988)
2. Yegen, D., Varilci, A., Yılmazlar, M., Terzioglu, C., Belenli, I.: Physica C **466**, 5 (2007)
3. Karaca, I., Celebi, S., Varilci, A., Malik, A.I.: Supercond. Sci. Technol. **16**, 100 (2003)
4. Varilci, A., Altunbas, M., Gorur, O., Karaca, I., Celebi, S.: Phys. Status. Solidi A **194**, 206 (2002)
5. Mihalache, V., Aldica, G.: J. Optoelectron. Adv. Mater. **9**, 919 (2007)
6. Guldeste, A., Goringe, M.J.: J. Cryst. Growth **257**, 129 (2003)
7. Chanda, B., Dey, T.K.: Magn. Supercond. Mater. **A–B**, 295 (2000)
8. Okada, M.: Supercond. Sci. Technol. **13**, 29 (2000)
9. Runde, M.: IEEE T. Appl. Supercon **5**, 813 (1995)
10. Godeke, A., Cheng, D., Dietderich, D.R., English, C.D., Felice, H., Hannaford, C.R., Prestemon, S.O., Sabbi, G., Scanlan, R.M., Hikichi, Y., Nishioka, J., Hasegawa, T.: IEEE T. Appl. Supercond. **18**, 516 (2008)
11. Miao, H., Meinesz, M., Czabai, B., Parrell, J., Hong, S.: AIP Conf. Proc. **986**, 423 (2008)
12. Biju, A., Aloysius, R.P., Syamaprasad, U.: Supercond. Sci. Technol. **18**, 1454 (2005)
13. Khalil, S.M.: Smart Mater. Struct. **14**, 804 (2005)
14. Ekicibil, A., Coskun, A., Ozcelik, B., Kiymac, K.: J. Low Temp. Phys. **140**, 105 (2005)
15. Li, Y., Kaviraj, S., Perkins, G.K., Driscoll, J., Caplin, A.D., Cao, G.H., Wang, B., Wei, L., Zhao, Z.X.: Physica C **355**, 51 (2001)
16. Fujii, H., Hishinuma, Y., Kitaguchi, H., Kumakura, H., Togano, K.: Physica C **331**, 79 (2000)
17. Aksan, M.A., Yakinci, M.E., Kadowaki, K.: J. Supercond. Nov. Magn. **23**, 371 (2010)
18. Bilgili, O., Selamet, Y., Kocabas, K.: J. Supercond. Nov. Magn. **21**, 439 (2008)
19. Malachevsky, M.T., Dovidio, C.A.: Supercond. Sci. Technol. **18**, 289 (2005)
20. Lim, H.J., Byrne, J.G.: Physica B **229**, 294 (1997)
21. Ren, Y., Weinstein, R., Liu, J., Sawh, R.P., Foster, C.: Physica C **251**, 15 (1995)
22. Ikuta, H., Mase, A., Yanagi, Y., Yoahikawa, M., Itoh, Y., Oka, T., Mizutani, U.: Supercond. Sci. Technol. **11**, 1345 (1998)
23. Xu, X.Q., Cai, Y.Q., Yang, C.X., Yao, X., Xu, S., Kortyka, A., Puzniak, R.: Supercond. Sci. Technol. **22**, 015001 (2009)
24. Xu, Y., Izumi, M., Tsuzuki, K., Zhang, Y.F., Xu, C.X., Murakami, M., Sakai, N., Hirabayashi, I.: Supercond. Sci. Technol. **22**, 095009 (2009)
25. Chevalier, B., Lepine, B., Lalerzin, A., Darriet, J., Eournau, J., Tarascon, J.M.: Mater. Sci. Eng. B **2**, 277 (1989)
26. Jayaram, B., Lanchester, P.C., Weller, M.T.: Physica C **160**, 17 (1989)
27. Coskun, A., Ekicibil, A., Ozcelik, B., Kiymac, K.: Chin. Phys. Lett. **21**, 2041 (2004)
28. Chen, D.X., Nogues, J., Rao, K.V.: Cryogenics **29**, 800 (1989)
29. Gomory, F., Lobotka, P.: Solid State Commun. **66**, 645 (1988)
30. Bean, C.P.: Rev. Mod. Phys. **36**, 31 (1964)
31. Clem, J.R.: Physica C **153–155**, 50 (1988)
32. Muller, K.H.: Physica C **159**, 777 (1989)
33. Literature of AC Susceptometer Model ACS 7000. Lakeshore Cryotronics, Inc., USA
34. Abd-Shukor, R., Das Arulsamy, A.: J. Phys. D, Appl. Phys. **33**, 836 (2000)
35. Kuzmin, Y.I.: Phys. Rev. B **64**, 094519 (2001)
36. Varilci, A., Yegen, D., Tassi, M., Stamopoulos, D., Terzioglu, C.: Physica B **404**, 4054 (2009)

37. Hein, R.A.: Phys. Rev. B **33**, 7539 (1986)
38. Adam, M.I.: Physica C **463**, 439 (2007)
39. Muller, K.H., Collocott, S.J., Driver, R.: Physica C **191**, 339 (1992)
40. Goldfarb, R.B., Leirental, M., Thomson, C.A.: In: Hein, R.A., Francavilla, T.L., Liebenberg, D.H. (eds.) Magnetic Susceptibility of Superconductors and Other Spin Systems, pp. 49–81. Plenum, New York (1991)
41. Terzioglu, C., Aydin, H., Ozturk, O., Bekiroglu, E., Belenli, I.: Physica B **403**, 3354 (2008)
42. Kong, W., Abd-Shukor, R.: J. Supercond. Nov. Magn. **23**, 257 (2010)